Effects of interchain couplings on excitations in finite-length conducting polymer chains

1996 J. Phys.: Condens. Matter 8 2185

(http://iopscience.iop.org/0953-8984/8/13/010)

J. Phys.: Condens. Matter **8** (1996) 2185–2195. Printed in the UK

Effects of interchain couplings on excitations in finite-length conducting polymer chains

Shi-jie Xie

Department of Physics, Shandong University, Jinan, Shandong, 250100, People's Republic of China

Received 4 September 1995, in final form 14 December 1995

Abstract. In the framework of the tight-binding model, the effects of longitudinal as well as transverse coupling between polyacetylene chains with different lengths and the electron–electron interactions on excitations have been studied. A new spinless charged polaronic excitation ($q = \pm e, s = 0$) was obtained due to the transverse interchain coupling, which is different from the general magnetic polaron ($q = \pm e, s = 1/2$) obtained in the perfect one-dimensional model. Due to its end positioning, a polaron is more easily stimulated energetically in a longer chain than in a shorter one, and it can hop to the longer chains nearby via either transverse or longitudinal interchain coupling. In addition, the transverse coupling decreases the energy of creation of a polaron. Considering the strong electron–electron interactions and the end positioning of chains in actual materials, we concluded that the one-dimensional model of conducting polymers is fairly appropriate in certain circumstances.

1. Introduction

The one-dimensional treatment of conjugated polymers has achieved some notable successes, including accounting for *t*-PA being a semiconductor rather than a metal, and predicting the existence and properties of solitons, polarons and bipolarons in *t*-PA [1, 2]. Most previous work idealizes polyacetylene as an infinite, highly conjugated one-dimensional hydrocarbon chain network, as illustrated in figure 1(a). However, in actual polymer samples, there are interactions between chains, such as the transverse interchain coupling between nearest parallel chains (figure 1(c)), which is weak (Vogl and Campbell obtained $t_\perp = 0.12$ eV from first-principles calculations for the three-dimensional *trans*-polyacetylene structure [3]) but is expected to have some importance. For example, the stability of polarons in *t*-PA has been questioned as a result of consideration of interchain coupling. On the basis of calculations for polarons in the Holstein molecular crystal model (MCM) [4], it was suggested that the interchain coupling is too strong in conducting polymers for a polaron to be stable [5, 6]. Nevertheless, Blackman and Sabra [7] did a numerical study based on an extended Su–Schrieffer–Heeger model [8] of the effects of interchain coupling on both the degenerate and nondegenerate conjugated polymers and showed that there is a discontinuous change in the degree of delocalization at a critical value of the coupling. A polaron is still stable in the case where the interchain coupling strength is smaller than a critical value ($t_\perp^c$). Recently, Mizes and Conwell [9] have also made tight-binding calculations of the atomic displacements and energy levels resulting from the addition of an electron to a pair of parallel *t*-PA chains and to a cluster of *t*-PA chains in the actual herringbone structure.

0953-8984/96/132185+11$19.50

In all of these studies, the electron–electron (e–e) interactions and the role of doped counter-ions have been totally neglected. My co-workers and I [2, 10] predicted that e–e interactions can cause the transition between polarons and bipolarons. Cruz and Phillips [11] made a more detailed study of the role of on-site (U), nearest-neighbour (V), and bond repulsion (W) of e–e Coulomb interactions. Further studies of the pinning effects of doped counter-ions on solitons and polarons in t-PA from a dilute to a strong doping concentration were reported in [12, 13, 14, 2], and predicted that the energy bands, the creation energy and the stability of a soliton or a bipolaron will be altered by the interactions between π-electrons and the counter-ions.

Moreover, most calculations have been for chains with the same lengths in periodic boundary conditions or with infinite lengths. In actual samples, however, there are chain breaks and various conjugation defects—such as sp^3 bonds, cross-links, inclusions of a catalyst or of a precursor polymer—that act as chain breaks. For t-PA, analysis of Raman scattering results has provided good evidence that a sizable proportion of chains have 40 or fewer C–H links [15]. Photoluminescence studies of thermally isomerized t-PA samples have also led to the conclusion that the mean lengths of t-PA segments are probably less than 26 C–H links [16]. Lanzani *et al* [17] employed a cw photomodulation technique and studied the excitations in soluble polyacetylene with controlled conjugation lengths. Jeyadev and Conwell [18] studied the properties of t-PA with sp^3 defects theoretically, using the method of modified neglect of differential overlap (MNDO). Recently, Misurkin *et al* [19] indicated that in real materials the polymer chains are always broken by the chain defects into conjugated fragments of finite lengths. In these cases, the neighbouring fragments are connected by resonance interactions. The effects of the resonance interactions and transverse interactions between t-PA chains of any length on excitations are, however, still to be established. In this paper, we propose two kinds of interchain coupling: one is the longitudinal coupling between two neighbouring fragments through their nearest ends, while the other is the transverse site-to-site coupling between two parallel chains; we study their effects on polaron excitations. The interactions between chains of different lengths are described. The model Hamiltonian is described and the formulae are derived in section 2. The numerical procedures are presented in section 3; the results are also analysed in this section, and the effects of both transverse and longitudinal coupling on the formation of excitations are shown. Finally, in section 4, we summarize our conclusions.

2. The model and formulae

2.1. Longitudinal interchain coupling

Let us firstly consider two t-PA chains placed end to end, as illustrated in figure 1(b). The strength of the interaction between the two fragments is hard to establish, but it certainly depends upon the situation for the nearest ends of the chains. So we confine the interactions to the end sites and introduce effective-coupling factors β_e and β_K describing the coupling between sites M and $M+1$, i.e. the nearest ends of the two chains, separately for the transfer of π-electrons and for the coupling of σ-electrons. In the tight-binding model [20], the Hamiltonian is

$$H = \sum_{n,s}^{N-1} \beta_e(n) t_{n,n+1}(c^+_{n+1,s}c_{n,s} + c^+_{n,s}c_{n+1,s}) + \sum_{n}^{N-1} \beta_K(n)\frac{1}{2}K(u_{n+1}-u_n)^2 + \sum_{n}^{N-1} \beta'_K(n)K'(u_{n+1}-u_n). \tag{1}$$

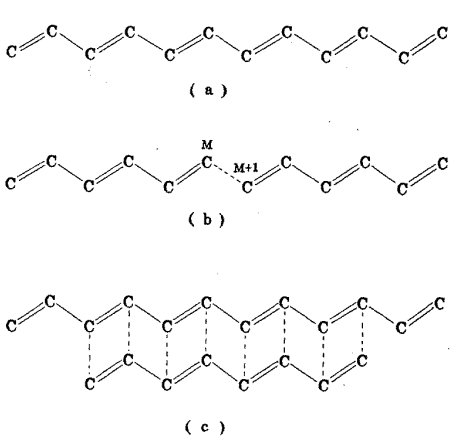

Figure 1. Schematic diagrams of the structure of polyacetylene: (a) a perfect 1D chain; (b) two chains coupled at their ends (longitudinal coupling); and (c) two chains coupled site by site (transverse coupling).

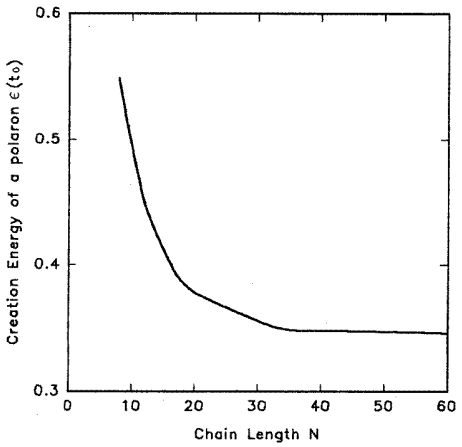

Figure 2. The dependence of the energy required for creation of a polaron on the length of a chain (free-end boundary conditions).

Here $t_{n,n+1} = t_0 - \alpha(u_{n+1} - u_n)$ [8]. t_0 is the transfer integral of π-electrons along each of the undimerized chains, α represents the electron–phonon coupling, u_n is the displacement of the (CH) group at site n, and K is the elastic constant. We have kept the numbering of the components of the two chains continuous, from the first chain to the second one, for convenience. The total number of (CH) groups in both chains is $N = N_1 + N_2$. In equation (1), the first term represents the energy of π-electrons and the second term represents the elastic energy. The last term is employed to stabilize the free ends of the chains and K' is a parameter to be determined later.

In the case of two t-PA chains with (CH) group numbers N_1 and $N_2 = N - N_1$, their end-coupling coefficients are defined as

$$\beta_e(n) = 1 - \beta_e\delta_{n,N_1} \qquad \beta_K(n) = 1 - \beta_K\delta_{n,N_1} \qquad \beta'_K(n) = 1 - \beta'_K\delta_{n,N_1} \tag{2}$$

where $\delta_{i,j}$ is the Kronecker delta function.

If $\beta_e = \beta_K = \beta'_K = 0$, we see from equations (1) and (2) that the two chains are united into one single chain [8, 10], while if $\beta_e = \beta_K = \beta'_K = 1$, the two chains become independent. These factors describe the longitudinal interchain coupling between t-PA fragments. It is easy to extend the model to a system of more chains coupled end to end.

For a small deviation from the equilibrium configuration, the static equilibrium condition can be derived, through second-order perturbation theory, by minimizing the total energy of the system

$$E = \sum_{\mu,s}{}' \varepsilon_\mu + \frac{1}{\pi\lambda}\sum_{n}^{N-1}\beta_K(n)(\phi_{n+1} + \phi_n)^2 + \frac{4}{\pi}\sum_{n}^{N-1}\beta'_K(n)k'(-1)^n(\phi_{n+1} + \phi_n) \tag{3}$$

which is

$$\phi_{n+1} + \phi_n = -2\lambda\lambda_1(n)(-1)^n k' + \pi\lambda\lambda_2(n)(-1)^n \sum_{\mu,s}{}' Z_{\mu,n+1}Z_{\mu,n} \tag{4}$$

where $\lambda_1(n) = \beta'_K(n)/\beta_K(n)$, $\lambda_2(n) = \beta_e(n)/\beta_K(n)$, $k' = (-\pi/4\alpha)K'$. The energy is measured in units of t_0. ϕ_n and λ are the dimensionless order parameter and the electron–phonon coupling introduced in [9]. The prime indicates summation over the occupied

electron states. ε_μ and $Z_{\mu,n}$ are the eigenvalue and eigenstate of the electrons, which are determined by the following eigenequation:

$$\begin{aligned}-\beta_e(n)(1-\delta_{n,N})[1+(-1)^n(\phi_{n+1}+\phi_n)]Z_{\mu,n+1}\\ -\beta_e(n-1)(1-\delta_{n,1})[1+(-1)^{n-1}(\phi_n+\phi_{n-1})]Z_{\mu,n-1}\\ =\varepsilon_\mu Z_{\mu,n}.\end{aligned} \tag{5}$$

Here the spin index s has been omitted.

For one isolated *trans*-PA chain with free ends, one can obtain from equation (4)

$$(-1)^{N-1}\phi_N-\phi_1=-2\lambda(N-1)k'+\pi\lambda\sum_{n,\mu,s}{}'^{N-1}Z_{\mu,n+1}Z_{\mu,n}$$

$$\begin{aligned}k'&=\frac{1}{2\lambda(N-1)}[\phi_1+(-1)^N\phi_N]+\frac{\pi}{N-1}\sum_{n,\mu}{}'^{N-1}Z_{\mu,n+1}Z_{\mu,n}\\ &=\int_0^{\pi/2}\frac{\cos^2\theta}{\sqrt{\cos^2\theta+4\phi_0^2\sin^2\theta}}\,\mathrm{d}\theta.\end{aligned} \tag{6}$$

The last expression is for an infinite-length dimerized chain with the dimensional dimerization parameter $\phi_n=\phi_0$. $k'=1$ or $K'=-4\alpha/\pi$ is obtained for the undimerized uniform structure with $\phi_0=0$ [21, 22].

2.2. Transverse interchain coupling

The transverse interchain coupling or 3D character of the t-PA structure is reflected if one considers the π-electron transfer integral perpendicular to the chain direction:

$$H_\perp=-\sum_{n_1,n_2,s}t_\perp(c^+_{n_1,s}c_{n_2,s}+c^+_{n_2,s}c_{n_1,s}) \tag{7}$$

where n_j is the corresponding site index of chain j as illustrated in figure 1(c). For the two-chain system, it was assumed that every C atom, rather than every other one, is coupled to its opposite neighbour on the other chain. It is easy to extend this model to a cluster of t-PA chains in the actual herringbone structure.

By minimizing with respect to ϕ_{nj} the total energy of the C positions, which are allowed to relax parallel to the chain, one can obtain the stationary equilibrium condition in the same way:

$$\phi_{n_j+1}+\phi_{n_j}=-2\lambda(-1)^{n_j}+\pi\lambda(-1)^{n_j}\sum_{\mu,s}{}'Z_{\mu,n_j+1}Z_{\mu,n_j} \tag{8}$$

where the eigenstate $Z_{\mu,n}$ and the corresponding eigenvalue ε_μ are determined by the following eigenequation:

$$\begin{aligned}-\Delta_1(n)[1+(-1)^n(\phi_{n+1}+\phi_n)]Z_{\mu,n+1}-\Delta_1(n-1)[1+(-1)^{n-1}(\phi_n+\phi_{n-1})]Z_{\mu,n-1}\\ -\Delta_2(n+N_{12}-N_1-1)\,t_\perp Z_{\mu,n+N_{12}-N_1-1}-\Delta_2(n)\,t_\perp Z_{\mu,n-N_{12}+N_1+1}\\ =\varepsilon_\mu Z_{\mu,n}\end{aligned} \tag{9}$$

where $\Delta_1(m)$ and $\Delta_2(m)$ are defined as

$$\Delta_1(m)=(1-\delta_{m,N_1})(1-\delta_{m,N_1+N_2}) \tag{10}$$

$$\Delta_2(m)=\begin{cases}1 & \text{if } N_{12}\leqslant m\leqslant N_{12}+N_2-1\\ 0 & \text{otherwise}\end{cases} \tag{11}$$

and N_{12} is the first position on the first chain from which the two chains begin to couple site to site. We have numbered the two chains continuously from the beginning of the first to the end of the second and assumed $N_1 \geqslant N_2$ for convenience. Mizes' situation (see [9]) can be recovered by setting $N_1 = N_2$.

Equations (4) and (5) or equations (9) and (10) are solved separately through numerical iteration for a given electron–phonon coupling parameter λ ($\lambda = 0.24$ for polyacetylene [1]). First, a starting lattice configuration ϕ_n is assumed for each chain. Then the eigenvalues and eigenstates are obtained from the eigenequation. Substituting the eigenstates into the equilibrium condition, a new lattice configuration is obtained. After repeating this process until the difference between the values of $\phi_{n+1} + \phi_n$ for two successive iterations is smaller than 10^{-5} for each n in each chain, the iteration stops.

3. Calculations and discussion

First, we checked the boundary effect on polarons in one fragment or isolated finite-length chain. In the case where the chain is doped with one donor or acceptor electron, one singly charged polaron is stimulated. Figure 2 shows the dependence of the creation energy of a polaron on the chain length. Although a stable polaron can form in a short chain, it was found that a high stimulation energy is required. For example, the creation energy of a polaron will increase onefold when the length of the chain decreases from $40a$ to $15a$. The iteration procedures show that a polaron is repelled into the inside of the chain by the ends, which act as potential walls. When the chain is longer than $40a$, the localization and the creation energy of a polaron become independent of the chain length. Similar results were obtained for fixed-end boundary conditions.

Now we consider the longitudinal coupling of the neighbouring chains. For simplicity of calculation, we just take $\beta_e = \beta_K = \beta'_K = \beta$, which corresponds to $\lambda_1(n) = \lambda_2(n) = 1 - \delta_{n,N_1}$. The stimulating process begins with one chain doped, and the other chain left neutral. If there is an external electric field along the direction of the chains, it can be seen that the doping-induced charged polaron will move from chain to chain through the longitudinal coupling, which goes beyond the scope of the present work. In the absent case of an external field, it was found that a polaron can be stimulated and remain steadily in the doped chain only when the chain is longer than a polaron width (about $14a$). The end–end coupling has little effect on the formation and stability of the polaron. But when the chains are short, for two equivalent chains the polaron will show a greater tendency towards being located at the end-linking position as the end–end coupling increases. The calculated lattice configurations for $N_1 = N_2 = 12$ with a series of values of β are shown in figure 3.

We now consider two chains with different lengths. If at the start the doped electron is inserted into the shorter chain, it is found that the stimulated polaron has a tendency to move towards the longer chain. For example, when the shorter chain consists of 10 (CH) groups, if $\beta > \beta_c = 0.19$ the final stationary state of the charged two-chain system is that in which the polaron is localized stably in the longer chain no matter where the polaron stimulation at the outset occurs. This phenomenon indicates the instability of polarons in shorter chains and polaron stimulation near the ends. The critical value β_c reflects the whether or not it is possible that a polaron could exist stably in a given short t-PA chain. Figure 4 gives the dependence of β_c on the length of the shorter chain. It can be seen that it is difficult to induce a stable polaron to form in a chain shorter than $8a$: it would hop to the longer chains nearby through the end–end interactions of the chains. Hence the end–end coupling should be considered in studying large polarons when chains are as short as a few lattice constants.

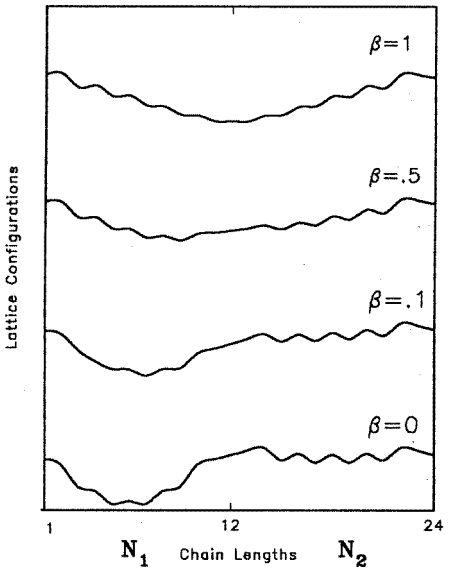

Figure 3. Lattice configurations of two chains coupled at their ends (longitudinal coupling).

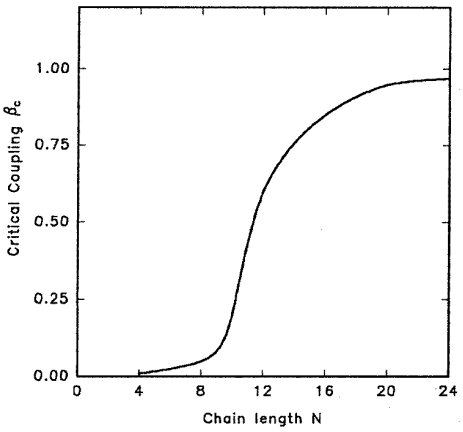

Figure 4. The dependence of the critical longitudinal coupling β_c on the length of the shorter chain.

Transverse coupling reflects the three-dimensional structure of polyacetylene. There have recently been a series of studies of two chains with the same lengths. Here we focus on the interchain coupling of two chains with different lengths as illustrated in figure 1(c). To discover the role of the boundaries, free-end boundary conditions were employed for both chains and one of the chains was designed to be very short. The calculations were performed on the first chain with $N_1 = 40, 20, 12$ and 8 and the second chain with $N_2 = 40, 80$ and 200 ($40a$ is long enough compared with the width of a polaron). The process began with one electron initially inserted into the shorter chain (chain I), leaving the longer chain (chain II) neutral. Then the final equilibrium state was reached through the numerical iteration of equations (9) and (10). The configurations of the chains are shown separately in figure 5 for $N_1 = N_2 = 20$ and in figure 6 for $N_1 = 20$, $N_2 = 40$. The site charge densities

$$Q(n_j) = \sum_{\mu,s}{}' |Z_{\mu,n_j,s}|^2 \tag{12}$$

are also shown in the figures. In fact, the strengths of the charged-polaron amplitude and the charge density at each site correspond with each other. One sees that the stimulated polaron will dislocate between the chains due to the interchain coupling, and the excess electronic charge will also redistribute between the chains. In the case of two chains with the same lengths (figure 5), the stimulation process causes a proportion of the charge of the excess electron initially in the first chain to begin to transfer to the second chain, which is neutral—so having a uniform dimerized structure at the beginning. This kind of transfer goes on steadily with the increasing of the interchain coupling until $t_\perp$ reaches a critical value $t_\perp^c$. Then the charges in the two chains reach the same value and they remain unchanged even if $t_\perp$ increases beyond the critical value. Correspondingly, the lattice configuration in each chain changes with the charge transfer. The amplitude of the polaron initially located in the first chain decreases, and a small 'polaron' appears in the second chain. Finally, the two 'polarons' become symmetric, with the same dip or amplitude, each having half of an

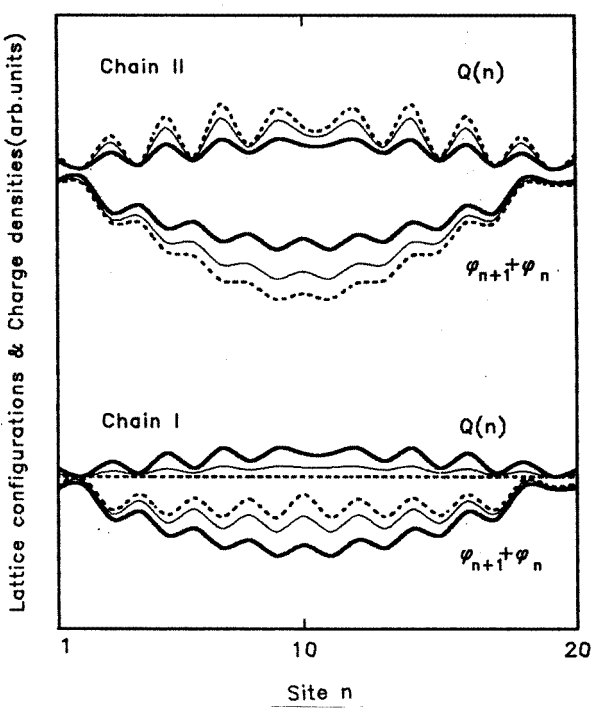

Figure 5. Lattice configurations and excess electronic charge distributions of two equivalent chains coupled site by site (transverse coupling). A polaron will dislocate between the chains with the increase of the interchain coupling. Key: $t_\perp = 0$ (dashed line); $t_\perp = 0.075t_0$ (solid line); and $t_\perp = 0.125t_0$ (narrow solid line). $N_1 = N_2 = 20$.

electron charge. Similar conclusions were obtained in [7] and [9].

In the case where the two chains are different in length—as shown in figure 6—the boundary positioning of the shorter chain becomes more apparent and strict, which is unfavourable to the formation of a polaron. We found that the excess electron (or the charged polaron) initially in the shorter chain will hop in its entirety to the longer chain once an interchain coupling exists, even though the coupling strength may be weak. This kind of transfer of electronic charges from shorter chains to longer chains results from the instability of polarons in shorter chains. However, with the increase of the coupling strength $t_\perp$, a small 'polaron' appears again in the shorter chain until the two 'polarons' in both chains have about the same dip or amplitude. But in this case, the critical coupling value $t_\perp^c$ is much higher than the value that Mizes obtained (see [9]). This process can be seen more clearly through the variations of the total excess charges in each of the chains with $t_\perp$, which are shown in figure 7. The dashed line shows the situation where the chains have the same lengths, while the solid line shows the situation where $N_1 = 20$ and $N_2 = 40$. These indicate that in the framework of one-dimensional structure or inclusion of a weak interchain coupling, the existence of chain ends can stabilize polarons in longer chains. With the increasing of the interchain coupling, a polaron will dislocate among the chains in the three-dimensional direction. In this case, a 3D model is necessary to describe conducting polymers.

Further, we consider the case where each chain is doped with one donor (or acceptor)

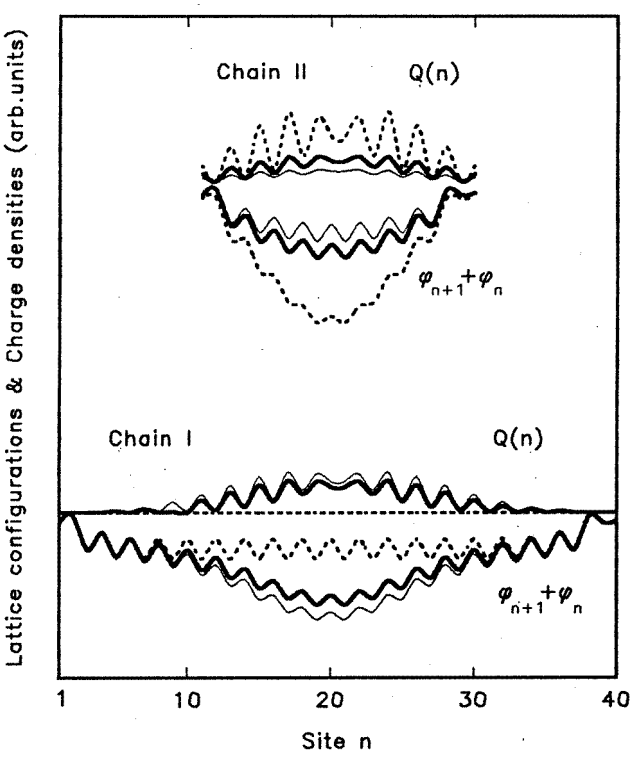

Figure 6. Lattice configurations and excess electronic charge distributions of two chains with different lengths, coupled site by site (transverse coupling). A polaron will firstly transfer to the longer chain and then dislocate between the chains with the increase of the interchain coupling. Key: $t_\perp = 0$ (dashed line); $t_\perp = 0.075t_0$ (solid line); and $t_\perp = 0.125t_0$ (narrow solid line). $N_1 = 20$ (up); $N_2 = 40$ (down).

electron. If there is no interchain coupling, it is well known that a charged polaron with spin 1/2 can form in each chain. But the existence of the interchain coupling makes a difference. The interchain coupling forms a bridge between the π-electrons in the chains and it makes the polarons in different chains interact. It was found that this kind of interaction will lead to the formation of a new charged polaronic excitation. It has one electronic charge but has no spin. The configuration and corresponding excess charge distribution of this kind of polaron, which is located in each chain, are shown in figure 8 (the up and down spins separately contribute half of an electronic charge to the polaron), while the creation energy versus interchain coupling is shown in figure 9. Similarly, for the magnetic polaron ($q = \pm e, s = 1/2$), it was found that the transverse interchain coupling makes the creation energy decrease.

In addition, we studied the effects of electron–electron (e–e) interactions on the critical transverse coupling value $t_\perp^c$. A simple Hubbard model was adopted:

$$H_{e-e} = U \sum_{n=1}^{N} c_{n,\uparrow}^{+} c_{n,\uparrow} c_{n,\downarrow}^{+} c_{n,\downarrow} \tag{13}$$

and it was treated in the Hartree–Fock approximation. In the one-polaron case, e–e interactions break the energy degeneracy for both spins. So we obtained energy levels

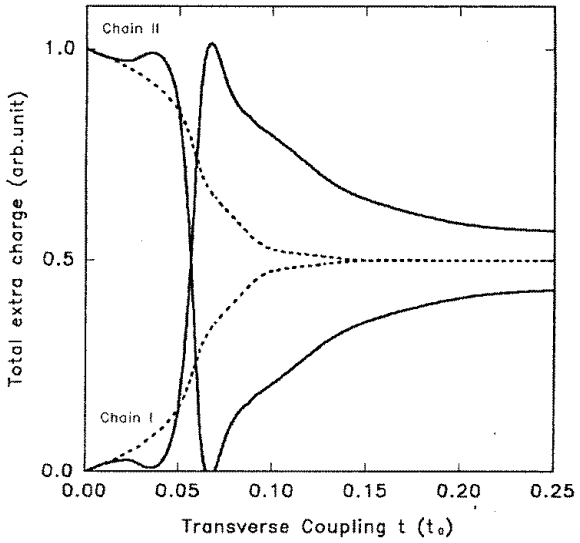

Figure 7. Dependencies of the total excess electronic charges in each of the chains on the transverse coupling factor $t_\perp$. $N_1 = N_2 = 40$ (dashed line); $N_1 = 20$ and $N_2 = 40$ (solid line).

for the spin up and the spin down separately. The total excess charges in each of the chains versus the e–e interaction U are shown in figure 10. One sees that with the increase of the e–e interaction strength U, the doped electron charge is more favourably located in one chain than for the case where $U = 0$. This shows that e–e interactions restrain the charge transfer between chains. It was also found that the spinless charged polaron is still stable within $U = 2.0t_0$.

4. Conclusion

Interchain couplings are of utmost importance for the high conductivity of conjugated polymers. In this paper, we have studied the effects of both longitudinal and transverse interchain couplings on excitations such as polarons in *t*-PA. The end positionings are of special importance. It was shown that, in actual samples, a polaron stimulated initially in a shorter chain can hop to the longer chains nearby through either the longitudinal end–end coupling or the transverse site–site coupling. The end–end coupling proposed here might also be used to describe a bond involving a defect to some extent, which would be of much more physical significance. For the transverse coupling, our calculations revealed the effect of interchain coupling on polarons between two chains with any lengths. The conclusion is that in actual polyacetylene samples, the chain lengths are not the same but have a distribution, and the existence of shorter chains and the electron–electron interactions restrain the electron transfer between chains. So the general 1D treatment of conducting polymers is applicable to some extent. Although only two-chain couplings are included here, it is straightforward to extend the model to a system of many-chain couplings. In addition, at a higher doping concentration, we obtained a new kind of charged polaron, which has one single electronic charge but has no spin. This new kind of excitation results from the transverse interchain coupling; it is different from the magnetic polaron obtained in perfect one-dimensional chains.

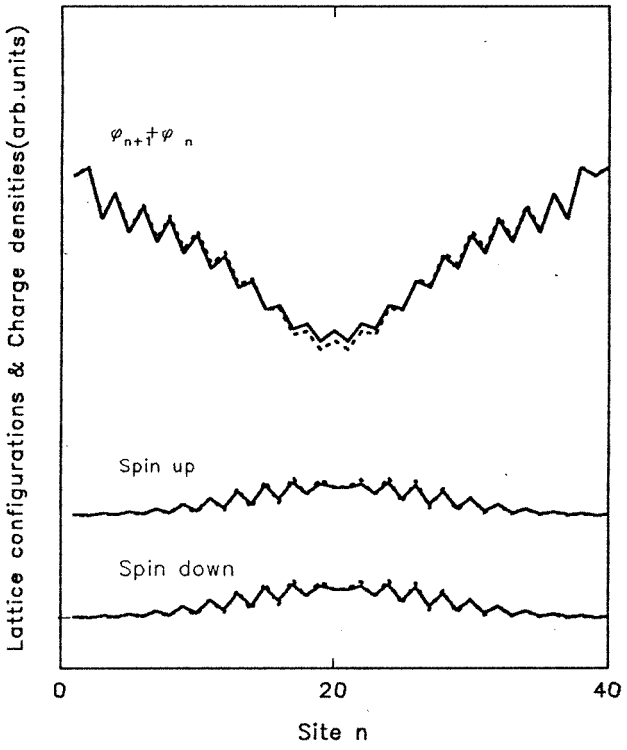

Figure 8. The lattice configuration (a polaron) and the corresponding electronic charge distributions for spin up and down in one chain ($t_\perp = 0.05$), for $U = 0$ (dashed line) and $U = 1.0t_0$ (solid line).

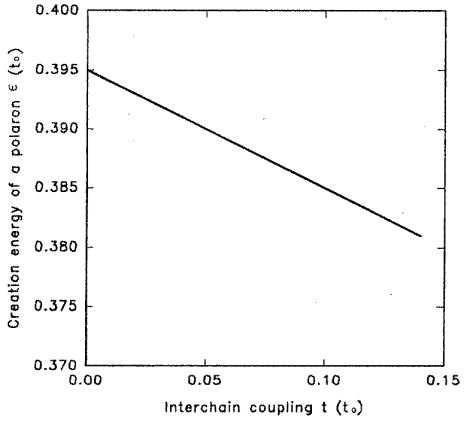

Figure 9. The dependence of the energy required for the creation of a spinless charged polaron on the interchain coupling strength $t_\perp$.

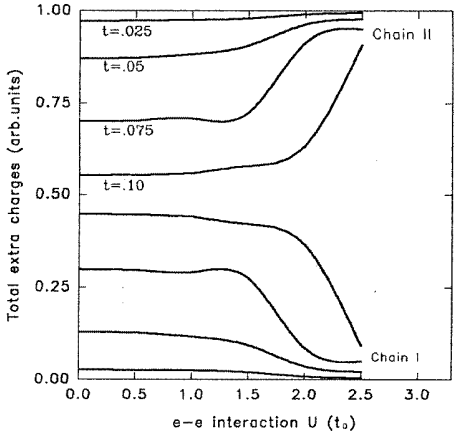

Figure 10. The dependences of the total excess charges in each of the chains on the e–e interaction U. (Transverse interchain coupling t; $N_1 = N_2 = 40$.)

Acknowledgments

The author thanks Professors L M Mei and X Sun for fruitful discussions.

References

[1] Heeger A J, Kivelson S, Schrieffer J R and Su W P 1988 *Rev. Mod. Phys.* **60** 781
[2] Xie S J and Mei L M 1994 *J. Phys. C: Solid State Phys.* **6** 3909
[3] Vogl P and Campbell D K 1990 *Phys. Rev.* B **41** 12 797
[4] Holstein T 1959 *Ann. Phys., NY* **8** 325
[5] Emin D 1986 *Phys. Rev.* B **33** 3973
[6] Gartstein Y N and Zakhidov A A 1986 *Solid State Commun.* **60** 105
[7] Blackman J A and Sabra M K 1993 *Phys. Rev.* B **47** 15 437
[8] Su W P, Schrieffer J R and Heeger A J 1980 *Phys. Rev.* B **22** 2099
[9] Mizes H A and Conwell E M 1993 *Phys. Rev. Lett.* **70** 1505
[10] Xie S J, Mei L M and Lin D L 1994 *Phys. Rev.* B **50** 13 364
[11] Cruz L and Phillips P 1994 *Phys. Rev.* B **49** 5149
[12] Stafstrom S and Bredas J L 1988 *Phys. Rev.* B **38** 4180
[13] Stafstrom S 1991 *Phys. Rev.* B **43** 9158
[14] Harigaya K, Wada Y and Fesser K 1990 *Phys. Rev.* B **42** 1268, 1276, 11 303; 1992 *Phys. Rev.* B **45** 4479
[15] Brivio G D and Mulazzi E 1984 *Phys. Rev.* B **30** 676
[16] Carter P W and Porter J D 1991 *Phys. Rev.* B **43** 14 478
[17] Lanzani G, Dellepiane G, Borghesi A and Tubino R 1992 *Phys. Rev.* B **46** 10 721
[18] Jeyadev S and Conwell E M 1988 *Phys. Rev.* B **37** 8262
[19] Misurkin I A, Zhuraleev T S, Geskin V M, Gulbinas V, Pakalnis S and Butvilos V 1994 *Phys. Rev.* B **49** 7178
[20] Wang X, Campbell D K, Lin H Q and Vogl P 1991 *Synth. Met.* **43** 3567
[21] Su W P 1980 *Solid State Commun.* **35** 899
[22] Xie S J, Mei L M and Sun X 1993 *Phys. Rev.* B **47** 14 905